PCCP

Accepted Manuscript

ROYAL SOCIETY OF CHEMISTRY

www.rsc.org/pccp

A Propargylbenzene Dimer: C–H···π Assisted π–π Stacking

Aniket Kundu,‡ Saumik Sen‡ and G. Naresh Patwari*

Department of Chemistry,

Indian Institute of Technology Bombay,

Powai, Mumbai 400 076 India.

E-mail: naresh@chem.iitb.ac.in

‡ Equal contribution

Abstract

The propargylbenzene dimer was investigated using mass selected electronic and infrared spectroscopy in combination with quantum chemical calculations. The IR spectrum in the acetylenic C–H stretching region indicates that the two propargylbenzene units in the dimer are in almost identical environment. Calculated stabilization energies at various levels of theory predict that the anti-parallel structure is the most stable isomer. The observed spectra are assigned to π-stacked structures which incorporate C–H···π interaction. The SAPT0 energy decomposition analysis revels that electrostatics contributes around 35% while the rest is from dispersion. Comparison with the phenylacetylene and toluene dimer indicates that the higher stabilization energy of PrBz dimer can be attributed to the synergy between the π–π stacking and C–H···π interactions.

1. Introduction

Aromatic π–π stacking constitutes an important class of intermolecular interaction and is known to influence wide variety of phenomena in chemistry,[1] biology,[2] and material science.[3] The key challenges are to understand its strength, orientational preference and inter conversion to structures which are close in energy but not necessarily π-stacked. The prototypical benzene dimer, has been a subject of intense debate over the past two decades. Experimentally only the tilted T–shaped structure has been observed,[4] even though high-level *ab-initio* calculations indicate that parallel displaced π-stacked dimer is almost isoenergetic.[5] A recent report suggests that the free energy always favours the tilted T-shaped structure,[6] however has been questioned.[7] Electrostatic based Hunter-Sanders π–π stacking model suggests that electron donating substituent on one of the constituent and electron withdrawing substituent on the other will lead to favourable π–π stacking.[8] On the contrary, high-level *ab-initio* calculations suggest that any substitution, whether electron donating or electron withdrawing, will favour formation of π–π stacking.[9] Adding to the debate is the π–π stacking in hetero-aromatic molecules such as pyridine and others.[10] The bulk of the investigations on π–π stacking use theoretical methods and the role of dispersion vis-à-vis electrostatics is the one of the most pertinent question that is being addressed using a variety of theoretical methods.[11]

Experimental investigations on gas-phase π-stacked dimers provide an excellent opportunity to address electronic effects and can be compared directly with the ab-initio calculations. However such reports are sparse and only three instances of π-stacked homo-dimers of substituted benzenes are reported. The π-stacked homo-dimers reported in the literature are (1) 1,2-difluorobenzene, using Fourier transform microwave spectroscopy,[12] (2) anisole, using high-resolution electronic spectroscopy[13] and (3) phenylacetylene, using IR-UV double-resonance spectroscopy.[14] These three examples

illustrate the fact that π-π stacking is feasible irrespective of the nature of the substituent (electron withdrawing or electron donating). In fact, it has been shown that even substitution of methyl group on the benzene ring favours the formation of π-stacked dimer.[15]

To delineate the factors responsible for π–π stacking in benzene one of the experimental strategies that can be adapted is to investigate π–π stacking with minimum perturbation on the benzene and then extrapolate to zero perturbation. Under this strategy, propargylbenzene (3-phenyl-1-propyne; PrBz) would be an ideal choice to investigate π–π stacking due to the following reasons (a) the presence of an in-plane ethynyl group would be lower the conjugation than that in toluene and (b) the electron withdrawing nature of the ethynyl group on the C_α position would possibly compensate for the electron donating nature of the methyl group. The molecular structure of PrBz is shown in Fig. 1. Additionally, one of the interesting aspects of PrBz is that it combines the features of phenylacetylene and toluene. Herein, formation of a C–H···π assisted π–stacked PrBz dimer is demonstrated using combination of spectroscopy and *ab-initio* calculations.

2. Methods

(A) Experimental

The details of the experimental setup have been described elsewhere.[16] Spectra were acquired using two-stage Wiley-McLaren time-of-flight (TOF) mass spectrometer coupled with supersonic jet expansion technique. PrBz (Aldrich) kept at 25 ºC was doped in helium buffer gas at 4 atm and expanded through a 0.5 mm diameter pulsed nozzle (Series 9, Iota One; General Valve Corporation) operating at 10 Hz into a vacuum chamber operating at 10^{-6} Torr. The expanded molecular beam was crossed with the

frequency doubled output of a dye laser (Narrow Scan GR; Radiant Dyes) operating with the Coumarin-540A dye, pumped with third harmonic of a Nd:YAG laser (Brilliant-B; Quantel). Electronic excitation spectra were recorded using one-color resonant two-photon ionization (1C-R2PI) spectroscopic technique by monitoring the appropriate mass ion signal in the TOF mass spectrometer using a channel electron multiplier (CEM-KBL-25RS; Sjuts) and a preamplifier (SR445A; Stanford Research Systems). The signal from the CEM was digitized by a digital storage oscilloscope (TDS-1012; Tektronix), which is interfaced to a personal computer using a data acquisition program written in LabView. The integrated signal intensity is plotted against the wavelength to get the 1C-R2PI spectrum. The infrared spectra in the acetylenic C–H stretching region were obtained using ion-dip infrared (IDIR) spectroscopic technique.[17] In this technique a pulsed UV laser excites and the ensuing 1C-R2PI signal is monitored as a measure of the ground state population. Prior to the UV laser, an IR laser is introduced, and its wavelength is scanned. When the IR wavelength is resonant with a vibrational transition of the species, the IR absorption induces reduction of the population of the ground state, which is then detected as a decrease in the intensity ion signal intensity. The resultant spectrum is called or ion-dip infrared (IDIR) spectrum. In our experiments the source of tunable IR light is an idler component of a $LiNbO_3$ OPO (Custom IR OPO; Euroscan Instruments) pumped with an injection-seeded Nd:YAG laser (Brilliant-B; Quantel). The typical bandwidth of both UV and IR lasers is about 1 cm^{-1} and the absolute frequency calibration is within ±2 cm^{-1}.

(B) Computational

A detailed conformational search was carried by generating about 35 initial structures by taking snapshots from MM2 MD trajectory followed geometry optimization at M06-2X/aug-cc-pVDZ level of theory,[18*a*] which converged on to 15 structures. Geometry optimization was

followed vibrational frequency calculations at the same level of theory to evaluate the zero-point energies and the vibrational frequencies of the systems and to verify nature of the minima obtained (presence of imaginary frequencies). Single point calculations were carried out using ωB97X-D and B2PLYP-D3 functionals,[18b,19] and MP2 methods with aug-cc-pVDZ basis set. The stabilization energy was determined as the difference between the dimer energy and the sum of monomer energies. The calculated stabilization energies were corrected for the vibrational zero-point energy (ZPE) and the basis-set superposition error (BSSE) using counterpoise method. The BSSE correction was made after geometry optimization. A scaling factor of 0.9523 was chosen so as to match the experimental vibrational frequency of the PrBz monomer and the same scaling factor was used for the complexes. The analysis of the stabilization energies of various PrBz dimer structure was carried out using Symmetry Adapted Perturbation Theory (SAPT).[20] The simplest of SAPT approach. i.e. SAPT0 with cc-pVTZ basis set along with the cc-pVTZ-JKFIT basis for the Hartree-Fock and cc-pVTZ-RI basis for The SAPT procedure.[21] The density fitting approach was used to reduce the computational expense. The main advantage of SAPT calculations is that it allows for the separation of interaction energy (E_{SAPT0}) into physically well-defined components, such as those arising from the electrostatic (E_{elec}), induction (E_{ind}) dispersion (E_{disp}) and exchange (E_{exch}) as given in equation (1)

$$E_{SAPT0} = E_{elec}^{(10)} + E_{exch}^{(10)} + E_{ind}^{(20)} + E_{exch-ind}^{(20)} + E_{disp}^{(20)} + E_{exch-disp}^{(20)} \qquad (1)$$

The perturbative method SAPT0 treats the monomers at the Hartree–Fock level and then dissociates the overall intermolecular interaction energy into the different components using second-order perturbation theory. It has been found that the SAPT0 calculations with reasonable basis sets provide good estimates of stabilization energies.[21] In the present analysis the exchange-induction and exchange-dispersion terms will be included to the parent

induction and dispersion terms. Spin component scaled (SCS)-SAPT0 calculations were also carried out and the energy decomposition in this case is given by equation (2).[22]

$$E_{SCS-SAPT0} = E_{SAPT0} - E_{disp}^{(20)} + E_{SCS-disp}^{(20)} \quad (2)$$

The interaction between the two PrBz monomers in the P1, P3 and P4 structures was analysed by the topographical study of electron density using the atoms in molecules (AIM) approach.[23] In the present case the critical points of electron density distribution were obtained, characterized by the rank and trace of the Hessian matrix. A (3,-1) bond critical point (BCP) with a positive Laplacian for the electron density distribution at the BCP indicates the non-covalent interaction. The electronic energy density H_c, and its components, the local one electron kinetic energy density (G_c), and the local potential energy density (V_c), for the charge distribution at the BCP's were also calculated. Geometry optimization and frequency calculations were carried out using the GAUSSIAN 09 suite of programs,[24] SAPT0 calculations were carried out using PSI4 *ab-Initio* package,[25] and AIM analysis was carried out using AIM-2000 package.[26] The structures and the vibrations were visualized by ChemCraft.[27]

3. Results and Discussion

The electronic excitation spectrum of PrBz (Fig. 2) shows an intense band at 37578 cm^{-1} which corresponds to absorption from the zero point energy level of the ground state to zero point energy level of the first excited state, while the corresponding band for toluene occurs at 37477 cm^{-1}.[28] The electronic excitation spectrum for the PrBz dimer, also shown in Fig. 2, remains largely in the same wavelength region, however is considerably broadened. The broadening of the electronic transition can possibly be attributed to variety of factors such as (a) distributed Franck-Condon factors, which is important for the π-stacked structures due to presence of low frequency vibrations (b) multiple isomers and (c) excitonic coupling.[29]

IR spectra in the acetylenic C–H stretching region were selectively recorded for the PrBz and its dimer and the results are presented in Fig. 3. PrBz monomer shows a single band at 3336 cm^{-1} corresponding to the acetylenic C–H stretching vibration. Interestingly, the IDIR spectrum of the PrBz dimer (Fig. 3) also shows as single band at 3332 cm^{-1}. The appearance of a single band in the IDIR spectrum of the PrBz dimer indicates that the local environment around the acetylenic groups in both the monomeric units of the dimer is almost identical. This spectrum also indicates that formation of PrBz dimer minimally perturbs the acetylenic C–H group in each of the monomers.

Ab-initio/DFT calculations were used to interpret the vibrational spectrum to obtain the structure of PrBz dimer. A detailed conformational search resulted in 15 low energy structures at M06-2X/aug-cc-pVDZ level of theory, which are shown in Fig. 4. Table 1 lists ZPE and BSSE corrected stabilization energies at various levels of theory. The stabilization energies calculated at MP2 level are the highest, which can be attributed to overestimation of dispersion.[30] For the various density functionals the energies calculated at ωB97X-D level are the highest followed by M06-2X and B2PLYP-D3. The PrBz dimers can be generally classified into three sets of structures. The first set consists of structures which are π-stacked along with noticeable C–H···π interaction (P1, P2, P3, P4, P11), while the second set consists of structures which exclusively π-stacked (P5, P6, P7, P8, P9, P10, P13, P14) and the third set consists structures which do not have any π–π stacking interaction and show C–H···π interaction (P12 and P15). Most of the π–stacked structures differ in the relative orientation of the two propargyl groups on each of the monomer. The relative stabilization energies of the first set is higher than the second followed by the third set. Even though there is substantial variation in stabilization energies calculated at various levels of theory, the stabilization energy ordering of various structure at all levels of theory is almost the same.

The structure P1 is the global minimum at all levels of theory and is an anti-parallel π-stacked structure with zero dipole moment.

As stated earlier, the appearance of a single band in the IDIR spectrum of the PrBz dimer indicates that the local environment around the acetylenic groups in both the monomeric units of the dimer is identical. The vibrational frequency calculations indicate that any of the P1, P3, P4, P6, P7, P8, P11 and P13 structures could be possible for PrBZ dimer. Among these the structures P6, P7, P8, P11 and P13 can be ruled out as they are at least 2 kJ mol^{-1} or higher in energy at all levels of theory used in this work. We had recently shown that under similar experimental conditions only the structures which are within 1 kJ mol^{-1} of global minimum are populated.[31] Therefore it is reasonable to neglect all the structures which are above 2 kJ mol^{-1}. Consequently, only the structures P1, P3 and P4 are considered. Table S1 (See ESI) lists the stabilization energies at HF and electron correlation levels without counterpoise correction at B2PLYP-D3/aug-cc-pVDZ method. In all the cases the electron correlation plays dominant role for the stabilization of the complexes, particularly for the three observed structures P1, P3 and P4. All the three structures are π-stacked and differ only by relative orientation of the two PrBz molecules. The present experiments cannot distinguish between any of the three structures. Therefore we assign the observed PrBz dimer to be originating from the three structures P1, P3 and P4.

The energy decomposition for all the PrBz dimers (P1-P15) was carried out using cc-pVTZ basis set using the simplest truncated model (SAPT0) and the results are listed in Table 2. The SAPT0 interaction energies are marginally higher than the stabilization energies calculated at MP2/aug-cc-pVDZ level, while the SCS-SAPT0 interaction energies are comparatively lower than the stabilization energies calculated at M06-2X/aug-cc-pVDZ level. Further, the stabilization energies calculated at ωB97X-D /aug-cc-pVDZ level are lie between the SAPT0 and SCS-SAPT0 interaction energies. Furthermore, the stabilization

energies calculated at ωB97X-D /aug-cc-pVDZ level are comparable to the SCS-SAPT0 interaction energies. Fig. 5 shows the SAPT0 energy decomposition for the six lowest energy structures (P1–P6). The P1 structures maximizes the electrostatic and induction components, which can be attributed to the anti-parallel alignment of two dipoles. Among the stabilizing components for the P1, P3 and P4 structures, electrostatics contributes about 39-36% while the rest is from dispersion. For all the three structures P1, P3 and P4 there is correlation between the dispersion and exchange components. The sum of dispersion and exchange energies are also plotted in Fig. 5, which indicates that these two components compensate for each other, therefore the net stabilization can be arrived without including these two components.

Fig. 6 shows the molecular graphs following AIM (Atoms in Molecules) analysis for the P1, P3 and P4 dimers. The bond critical points (BCPs) indicate the presence of the both C···C (π–π stacking) and C–H···π interactions between the two monomers in all the three structures. The topological parameters are listed in Table 3 indicates interaction between closed shell molecules. The observed structures of the PrBz dimer (P1, P3 and P4) incorporate C–H···π interaction, which is well known for its stabilizing effect on in a variety of structures in chemistry and biology.[32] AIM calculations point out the presence of π–π stacking between the two acetylenic units in the P3 structure in addition to the π–π stacking interaction between the phenyl rings. In the case of P4 structure, the π electron density of the C≡C bond is also involved in π–π stacking and C–H···π interactions.

Since PrBz incorporates features of phenylacetylene and toluene it is only prudent to make a comparison between all the three dimers. The spectroscopy and the calculated structures of phenylacetylene dimer have been reported.[14,33] However, in order to make direct comparison calculations on phenylacetylene dimer were carried out at same level of theory. Six unique π-stacked structures were identified, which are depicted in Fig. 7. Further,

Table 4 lists the ZPE and BSSE corrected stabilization energies calculated at various levels of theory. Even in the case of phenylacetylene dimer the anti-parallel structure (PA1) is the most stable. The π-stacked structures of the phenylacetylene dimer are about 8-12 kJ mol^{-1} less stable than the π-stacked structures of PrBz dimer. This difference can be attributed to the existence of C–H···π interactions in the PrBz dimer, which are absent in the phenylacetylene dimer. In the case of toluene dimer the anti-parallel structure π-stacked structure which incorporates C–H···π interactions is the most stable, which has also been recalculated at the same level of theory used of PrBz dimer which enables direct comparison. The present set of calculations indicate that the stabilization energy of the toluene dimer is about 10-14 kJ mol^{-1} lower than the most stable observed PrBz dimer. It is interesting to note that at any level of calculation the stabilization energy of the most stable PrBz dimer (P1) is about 70% of the value obtained by the sum of stabilization energies of the most stable anti-parallel structures of the phenylacetylene and toluene dimers, even though PrBz dimer has only two benzene rings against four from phenylacetylene and toluene dimers. Therefore the stabilization of PrBz dimer can be attributed to the synergy between the π–π stacking and C–H···π interactions. The larger stabilization energy of PrBz dimer relative to phenylacetylene and toluene dimers can be attributed to larger cross-section of interaction for the PrBz dimer and displaced phenyl rings in the PrBz dimer allow the parallel interaction of aromatic C–H group with the C≡C bond.[34]

4. Conclusions

The IDIR spectrum of the PrBz dimer indicates that the local environment around the acetylenic groups in both the monomeric units of the dimer is identical with marginal change in observed C-H stretching frequency compared to PrBz monomer. Ab-initio and DFT calculations indicate that the anti-parallel structure is the most stable structure. The

broadening of the electronic excitation spectrum is attributed to several factors including formation of multiple isomers. The calculations indicate presence of three isomers with the energy band of 2 kJ mol^{-1}, which have been assigned to the observed PrBz dimer. The observed PrBz dimer forms π–stacked dimers incorporating C–H···π interactions as well. Dispersion plays a dominant role in formation of PrBz dimer with significant contribution from electrostatics. The displaced phenyl rings enhance the stability of PrBz dimer due to interaction between the aromatic CH group and π electron density of the C≡C bond.

Author contributions

The problem was formulated by GNP. AK carried out all the experiments and SS and carried out all the calculations. The results were interpreted jointly by AK, SS and GNP.

Acknowledgements

This material is based upon work supported by Board of Research in Nuclear Sciences (Grant No. 2012/34/14) and Department of Science and Technology (Grant No. SB/S1/PC-29/2012). Authors wish to thank Dr. G. Narahari Sastry and Dr. Debashree Ghosh for valuable discussions. A.K. and S.S. thank Department of Chemistry, IIT Bombay for teaching assistanceship. High performance computing facility of IIT Bombay is gratefully acknowledged. Thanks are also due to the reviewers, whose suggestions have considerably improved the manuscript**.**

Notes

Electronic Supplementary Information (ESI) available: Tables containing Hartree-Fock and Electron correlation parts of stabilization energies and Cartesian coordinates of all the structures. See DOI: 10.1039/c000000x/

References

1 (a) T. M. Parker, E. G. Hohenstein, R. M. Parrish, N. V. Hud and C. D. Sherrill, *J. Am. Chem. Soc*., 2013, **135**, 1306-1316. (b) Y.-Y. Zhou, J. Li, L. Ling, S.-H. Liao, X.-L Sun, Y.-X. Li, L.-J. Wang and Y. Tang, *Angew. Chem. Int. Ed*., 2013, **52**, 1452 -1456.

2 (a) K. M. Guckian, B. A. Schweitzer, R. X. F. Ren, C. J. Sheils, D. C. Tahmassebi and E. T. Kool, *J. Am. Chem. Soc*., 2000, **122**, 2213-2222. (b) G. B. McGaughey, M. Gagne and A. K. Rappe, *J. Biol. Chem*., 1998, **273**, 15458-15463. (c) S. K. Burley and G. A. Petsko, *Science*, 1985, **229**, 23-28.

3 (a) B. W. Greenland, M. B. Bird, S. Burattini, R. Cramer, R. K. O'Reilly, J. P. Patterson, W. Hayes, C. J. Cardin and H. M. Colquhoun, *Chem. Commun*., 2013, **49**, 454-456. (b) F. Schlosser, M. Moos, C. Lambert and F. Wurthner, *Adv. Mater*., 2013, **25**, 410-414.

4 (a) E. Arunan and H. S. Gutowsky, *J. Chem. Phys.*, 1993, **98**, 4294. (b) U. Erlekam, M. Frankowski, G. Meijer and G. von Helden, *J. Chem. Phys.*, 2006, **124**, 171101. (c) V. Chandrasekaran, L. Biennier, E. Arunan, D. Talbi and R. Georges, *J. Phys. Chem. A*, 2011, **115**, 11263. (d) M. Schnell, U. Erlekam, P. R. Bunker, G. von Helden, J-U. Grabow, G. Meijer and A. Ad van der Avoird, *Angew. Chem. Int. Ed*., 2013, **52**, 5180.

5 T. Janowski and P. Pulay, *Chem. Phys. Lett.*, 2007, **447**, 27. (b) R. A Distasio, G. von Helden, R. P. Steele and M. Head-Gordon, *Chem. Phys. Lett.*, 2007, **437**, 277. (c) E. C. Lee, D. Kim, P. Jurecka, P. Tarakeshwar, P. Hobza and K. S. Kim, *J. Phys. Chem. A*, 2007, **111**, 3446. (d) M. O Sinnokrot and C. D. Sherrill, *J. Am. Chem. Soc.,* 2004, **126**, 7690.

6 (a) A. K. Tummanapelli and S. Vasudevan, *J. Chem. Phys*., 2013, **139**, 201102. (b) A. K. Tummanapelli and S. Vasudevan, *J. Chem. Phys*., 2014, **140**, 227102.

7 A. van der Avoird, R. Podeszwa, B. Ensing and K. Szalewicz, *J. Chem. Phys*., 2014, **140**, 227101.

8 (a) C. A. Hunter and J. K. M. Sanders, *J. Am. Chem. Soc.*, 1990, **112**, 5525-5534. (b) C. A. Hunter, *Chem. Soc. Rev.,* 1994, **23**, 101-109.

9 (a) M. O. Sinnokrot and C. D. Sherrill, *J. Phys. Chem. A*, 2003, **107**, 8377-8379. (b) S. E. Wheeler and K. N. Houk, *J. Am. Chem. Soc.*, 2008, **130**, 10854.

10 (a) B. K. Mishra and N. Sathyamurthy, *J. Phys. Chem. A*, 2005, **109**, 6-8. (b) W. Wang and P. Hobza, *ChemPhysChem*, 2008, **9**, 1003-1009. (c) M. Guin, G. N. Patwari, S. Karthikeyan and K. S. Kim, *Phys. Chem. Chem. Phys*., 2011, **13**, 5514-5525.

11 S. Grimme, *Angew. Chem. Int. Ed*., 2008, **47**, 3430 -3434.

12 T. Goly, U. Spoerel and W. Stahl, *Chem. Phys.*, 2002, **283**, 289-296.

13 G. Pietraperzia, M. Pasquini, N. Schiccheri, G. Piani, M. Becucci, E. Castellucci, M. Biczysko, J. Bloino and V. Barone, *J. Phys. Chem. A,* 2009, **113**, 14343-14351.

14 S. Maity, R. Sedlak, M. A. Addicoat, S. Irle, P. Hobza and G. N. Patwari. *Phys. Chem. Chem. Phys*., 2011, **13**, 16706-16712; *Phys. Chem. Chem. Phys*., 2011, **13**, 21651-21652.

15 (a) D. M. Rogers, J. D. Hirst, E. P. F. Lee and T. G. Wright, *Chem. Phys. Lett*., 2006, **427**, 410-413. (b) S. Tsuzuki, K. Honda, T. Uchimaru and M. Mikami, *J. Chem. Phys*. 2005, **122**, 144323. (c) B. Ernstberger, H. Krause, A. Kiermeier and H. Neusser, *J. Chem. Phys*., 1990, **92**, 5285-5296

16 P. C. Singh and G. N. Patwari, *Curr. Sci*., 2008, **95**, 469-474.

17 (a) R. H. Page, Y. R. Shen and Y. T. Lee, *J. Chem. Phys.*, 1988, **88**, 5362-5376. (b) S. Tanabe, T. Ebata, M. Fujii and N. Mikami, *Chem. Phys. Lett.*, 1993, **215**, 347-352. (c) A. Fujii, G. N. Patwari, T. Ebata and N, Mikami, *Int. J. Mass. Spectrom.*, 2002, **220**, 289-312.

18 (a) Y. Zhao and D. G. Truhlar, *Theor. Chem. Acc.*, 2008, **120**, 215-241. (b) J. D. Chai and M. Head-Gordon, *Phys. Chem. Chem. Phys.*, 2008, **10**, 6615-6620.

19 L. Goerigk and S. Grimme, *J. Chem. Theory Comput.*, 2011, **7**, 291-309.

20 (a) B. Jeziorski, R. Moszynski and K. Szalewicz, *Chem. Rev.*, 1994, **94**, 1887-1930. (b) K. Szalewicz, *WIRES: Comput. Mol. Sci.*, 2012, **2**, 254-272.

21 E. G. Hohenstein, C. D. Sherrill, *J. Chem. Phys.*, 2010, **132**, 184111.

22 S. Grimme, *J. Chem. Phys.*, 2003, **118**, 9095-9102.

23 R. F. Bader, *Atoms in Molecules: A Quantum Theory*, Oxford University Press: Oxford, U.K., 1990.

24 M. J. Frisch, G. W. Trucks, H. B. Schlegel, G. E. Scuseria, M. A. Robb, J. R. Cheeseman, G. Scalmani, V. Barone, B. Mennucci, G. A. Petersson, H. Nakatsuji, M. Caricato, X. Li, H. P. Hratchian, A. F. Izmaylov, J. Bloino, G. Zheng, J. L. Sonnenberg, M. Hada, M. Ehara, K. Toyota, R. Fukuda, J. Hasegawa, M. Ishida, T. Nakajima, Y. Honda, O. Kitao, H. Nakai, T. Vreven, J. A. Montgomery, Jr., J. E. Peralta, F. Ogliaro, M. Bearpark, J. J. Heyd, E. Brothers, K. N. Kudin, V. N. Staroverov, R. Kobayashi, J. Normand, K. Raghavachari, A. Rendell, J. C. Burant, S. S. Iyengar, J. Tomasi, M. Cossi, N. Rega, J. M. Millam, M. Klene, J. E. Knox, J. B. Cross, V. Bakken, C. Adamo, J. Jaramillo, R. Gomperts, R. E. Stratmann, O. Yazyev, A. J. Austin, R. Cammi, C. Pomelli, J. W. Ochterski, R. L. Martin, K. Morokuma, V. G. Zakrzewski, G. A. Voth, P. Salvador, J. J. Dannenberg, S.

Dapprich, A. D. Daniels, O. Farkas, J. B. Foresman, J. V. Ortiz, J. Cioslowski and D. J. Fox, *Gaussian-09, Revision A.02* Gaussian, Inc., Wallingford CT, 2009.

25 (a) J. M. Turney, A. C. Simmonett, R. M. Parrish, E. G. Hohenstein, F. A. Evangelista, J. T. Fermann, B. J. Mintz, L. A. Burns, J. J. Wilke, M. L. Abrams, N. J. Russ, M. L. Leininger, C. L. Janssen, E. T. Seidl, W. D. Allen, H. F. Schaefer, R. A. King, E. F. Valeev, C. D. Sherrill and T. D. Crawford, *Wiley Interdisciplinary Reviews: Computational Molecular Science*, 2012, **2**, 556-565. (b) T. M. Parker, L. A. Burns, R. M. Parrish, A. G. Ryno and C. D. Sherrill, *J. Chem. Phys.*, 2014, **140**, 094106.

26 F. Biegler-Konieg, J. Schonbohm and D. Bayles, *J. Comput. Chem.*, 2001, **22**, 545-559.

27 http://www.chemcraftprog.com

28 J. B. Hopkins, D. E. Powers and R. E. Smalley, *J. Chem. Phys*., 1980, **72**, 5039-5048.

29 L. Muzangwa, S. Nyambo, B. Uhler and S. A. Reid, *J. Chem. Phys*., 2012, **137**, 184307.

30 K. E. Riley, M. Pitoak, P. Jurecka and P. Hobza, *Chem. Rev.,* 2010, **110**, 5023-5063.

31 A. Dey, S. I. Mondal and G. N. Patwari, *ChemPhysChem*, 2013, **14**, 746-753.

32 (a) M. Nishio, *Phys. Chem. Chem. Phys*., 2011, **13**, 13873-13900. (b) M. Nishio, Y. Umezawa, J. Fantini, M. S. Weiss and P. Chakrabarti, *Phys. Chem. Chem. Phys*., 2014, **16**, 12648-12683. (c) J. Vondrasek, L. Bendova, V. Klusak and P. Hobza, *J. Am. Chem. Soc.*, 2005, **127**, 2615-2619.

33 G. N. Patwari, P. Venuvanalingam, and M. Kołaski, *Chem. Phys*., 2013, **415**, 150-155.

34 D. B. Ninkovic, J. M. Andric, S. N. Malkov and S. D. Zaric, *Phys. Chem. Chem. Phys*., 2014, **16**, 11173-11177. (b) G. V. Janjic., D. Z. Veljkovic and S. D. Zaric, *Cryst. Growth Des.*, 2011, **11**, 2680-2683. (c) D. B. Ninkovic, G. V. Janjic, D. Veljkovic, D. N. Sredojevic and S. D. Zaric, *ChemPhysChem*, 2011, **12**, 3511-3514. (d) S. E. Wheeler, *J. Am. Chem. Soc*., 2011, **133**, 10262-10274.

Table 1. ZPE and BSSE corrected stabilization energies (kJ mol^{-1}), dipole moments (Debye) and the acetylenic C-H stretching frequencies (cm^{-1}) for various structures of PrBz dimer.

Structure	M06-2X	ωB97X-D	B2PLYP-D3	MP2	μ	ν_{C-H}
PrBz	-	-	-	-	0.49	3336
P1	-31.7	-33.6	-26.8	-37.7	0.00	3334
P2 (1)	-28.9	-32.6	-25.3	-36.1	0.59	3303, 3324
P3	-29.4	-32.3	-25.1	-34.9	0.89	3334
P4	-27.7	-32.0	-25.3	-36.8	0.30	3333
P5	-28.9	-31.3	-24.1	-35.1	0.39	3333, 3338
P6	-26.6	-30.4	-23.6	-34.8	0.17	3333, 3334
P7	-25.0	-28.8	-22.4	-34.1	0.52	3333
P8	-25.2	-28.7	-22.1	-34.1	0.69	3335
P9 (1)	-25.16	-28.6	-22.0	-33.5	0.82	3304, 3315
P10	-24.8	-28.0	-21.5	-32.5	0.83	3329, 3333
P11	-21.1	-24.3	-19.1	-27.4	0.69	3332, 3333
P12 (1)	-20.0	-22.7	-18.5	-23.7	0.49	3311, 3333
P13	-18.7	-20.6	-15.2	-25.9	0.00	3339
P14	-14.6	-17.6	-12.5	-18.5	0.58	3317, 3334
P15	-15.6	-16.6	-12.8	-17.3	0.41	3313, 3331

Number of imaginary frequencies are shown in parenthesis.

Table 2. SAPT0 interaction energy components (kJ mol^{-1}) for various structures of PrBz dimer.

Structure	E_{elec}	E_{ind}	E_{disp}	E_{exch}	E_{SAPT0}	$E_{SCS\text{-}disp}$	$E_{SCS\text{-}SAPT0}$
P1	-33.6	-9.3	-69.4	68.0	-44.4	-54.3	-29.2
P2	-32.1	-8.0	-70.3	70.3	-40.2	-55.0	-24.8
P3	-33.7	-8.3	-66.1	67.7	-40.4	-51.7	-26.0
P4	-31.9	-7.9	-71.0	70.8	-39.9	-55.5	-24.5
P5	-28.7	-8.1	-69.7	68.2	-38.4	-54.5	-23.2
P6	-26.8	-7. 9	-70.7	68.3	-37.0	-55.2	-21.6
P7	-26.5	-6.9	-71.2	69.2	-35.3	-55.7	-19.8
P8	-27.6	-7.0	-72.3	70.5	-36.3	-56.6	-20.6
P9	-27.8	-7.9	-68.9	69.6	-34.9	-53.9	-19.9
P10	-27.1	-7.1	-68.4	68.1	-34.5	-53.5	-19.6
P11	-23.7	-6.0	-51.7	50.7	-30.7	-40.4	-19.4
P12	-26.3	-7.6	-43.5	46.9	-30.6	-33.9	-21.0
P13	-15.8	-5.5	-63.5	59.1	-25.7	-49.6	-11.8
P14	-13.5	-4.9	-42.3	40.8	-19.9	-33.0	-10.6
P15	-21.9	-5.0	-36.2	41.4	-21.7	-28.3	-13.8

Table 3: Topological parameters at the intermolecular BCPs for the C···C and C–H···C(π) contacts for P1, P3 and P4 structures of the PrBz dimer calculated at M06-2X/aug-cc-pVDZ Level.

		Distance (Å)	ρ	$\nabla^2(\rho)$	G_b	V_b	H_b
P1	C···C	3.389	0.0061	0.0043	0.0037	-0.0031	0.0006
	C–H···C(π)	2.772	0.0077	0.0064	0.0054	-0.0045	0.0009
		2.752	0.0077	0.0062	0.0053	-0.0045	0.0008
		2.771	0.0077	0.0064	0.0054	-0.0045	0.0009
		2.751	0.0077	0.0062	0.0053	-0.0045	0.0008
		3.405	0.0052	0.0034	0.0029	-0.0024	0.0005
		3.355	0.0062	0.0043	0.0037	-0.0030	0.0007
P2	C···C	3.405	0.0052	0.0034	0.0029	-0.0024	0.0005
		3.355	0.0062	0.0043	0.0037	-0.0030	0.0007
		3.239	0.0073	0.0052	0.0043	-0.0035	0.0008
	C–H···C(π)	2.966	0.0063	0.0048	0.0038	-0.0029	0.0009
		2.794	0.0064	0.0051	0.0041	-0.0030	0.0011
		2.934	0.0067	0.0056	0.0046	-0.0037	0.0009
P3	C···C	3.444	0.0050	0.0033	0.0028	-0.0023	0.0005
		3.496	0.0062	0.0039	0.0033	-0.0028	0.0005
		3.296	0.0071	0.0047	0.0040	-0.0032	0.0008
	C–H···C(π)	2.762	0.0070	0.0051	0.0043	-0.0035	0.0008
		2.860	0.0063	0.0052	0.0041	-0.0030	0.0011
		2.948	0.0057	0.0044	0.0035	-0.0026	0.0009

Table 4. ZPE and BSSE corrected stabilization energies (kJ mol^{-1}) dipole moments (Debye) for various structures of phenylacetylene dimer and toluene dimer.

Structure	M06-2X	ωB97X-D	B2PLYP-D3	MP2	μ
PA1	-20.4	-22.3	-18.6	-29.4	0.00
PA2	-19.2	-21.7	-18.0	-29.0	0.77
PA3	-20.1	-21.5	-17.9	-29.7	0.94
PA4	-17.5	-20.2	-16.9	-26.4	1.11
PA5	-17.3	-19.6	-16.0	-26.2	1.24
PA6	-14.4	-15.2	-11.9	-22.2	0.00
TU1	-18.6	-21.0	-15.7	-25.2	0.00

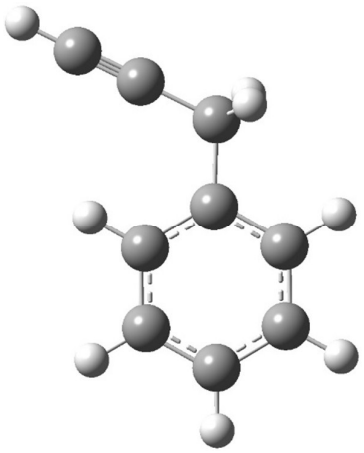

Fig. 1. The molecular structure of propargylbenzene (PrBz).

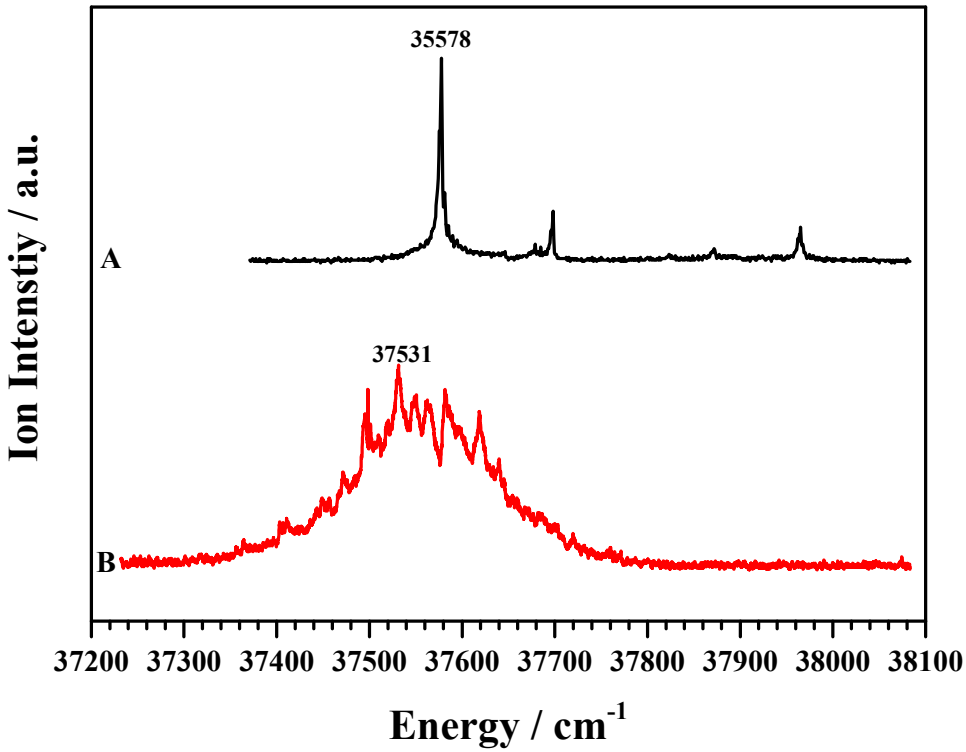

Fig. 2. The electronic spectra recorded using resonant two-photon ionization spectroscopic method for (A) PrBz and (B) PrBz dimer. The two spectra (A) and (B) were recorded by monitoring mass signals at 116 and 232 Da, respectively.

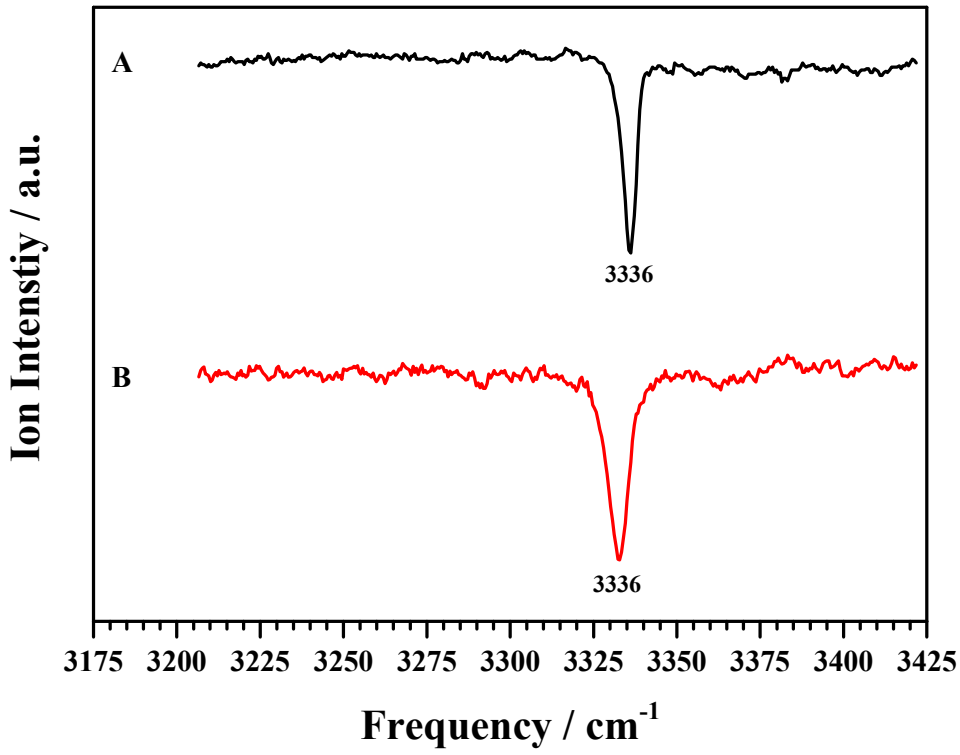

Fig. 3. The IDIR spectra in the acetylenic C–H stretching region for (A) PrBz and (B) PrBz dimer. The two spectra were recorded by monitoring mass signals at 116 and 232 Da, following selective excitation at 37588 and 37537 cm^{-1}, respectively.

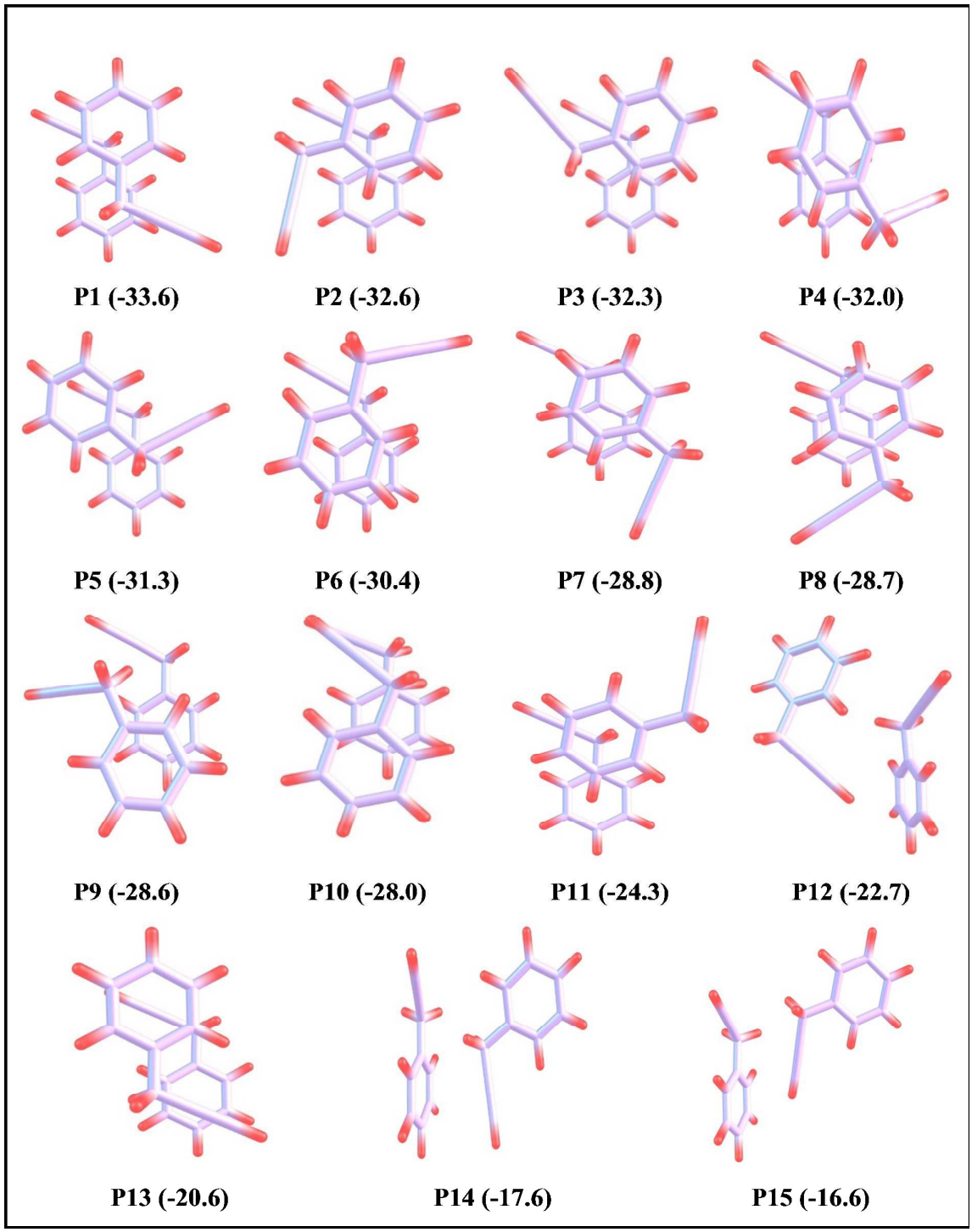

Fig. 4. Structures of PrBz dimer optimized at M06-2X/aug-cc-pVDZ level. ZPE and BSSE corrected stabilization energies (kJ mol^{-1}) at ωB97X-D/aug-cc-pVDZ level of theory are shown in parenthesis (see Table 1).

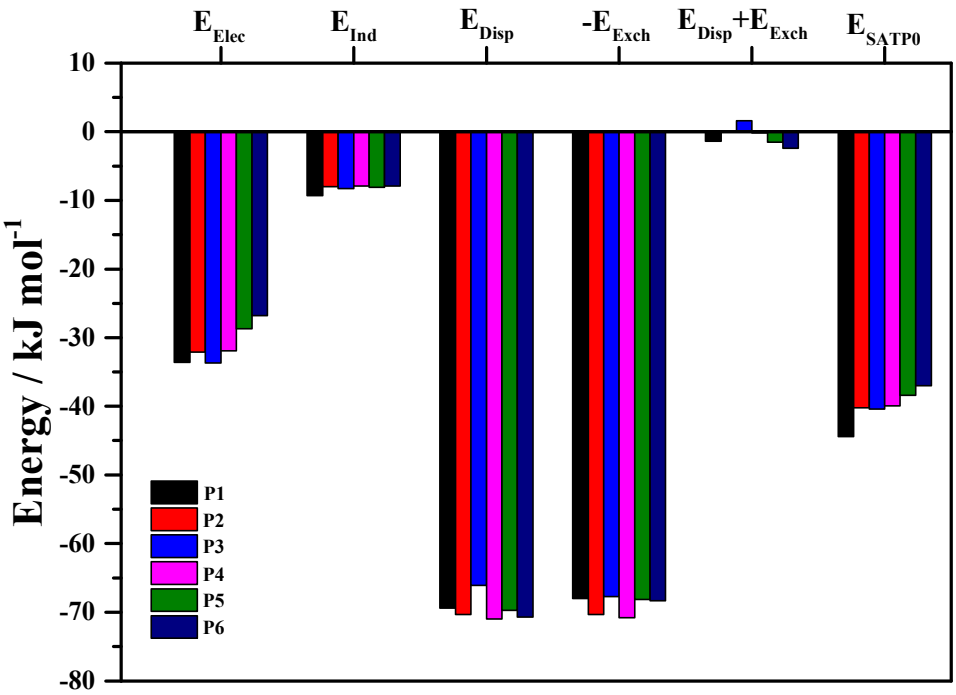

Fig. 5. SAPT0 energy partitioning for the six lowest energy structures (P1–P6) of PrBz dimer (see Table 2).

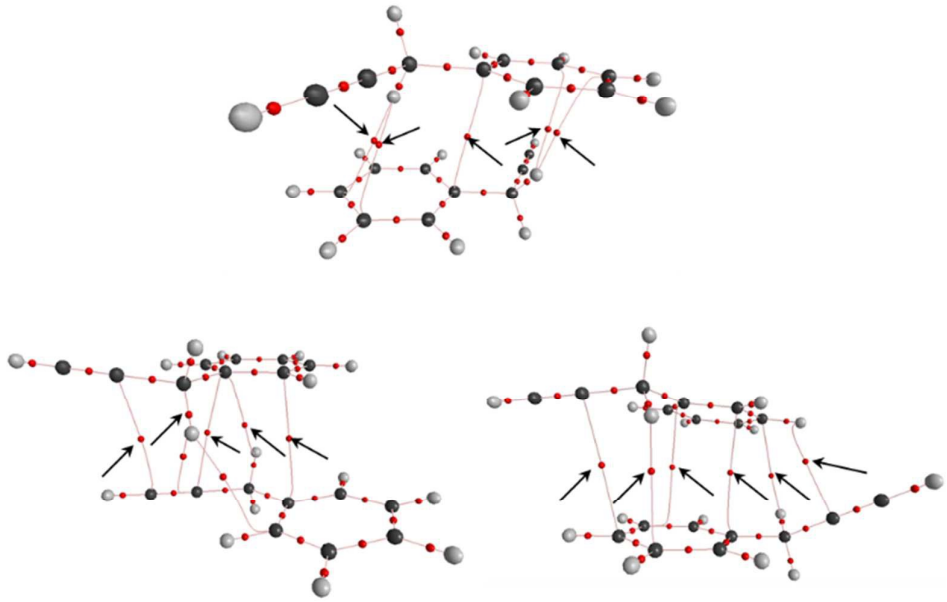

Fig. 6. Molecular graphs for PrBz dimer structures P1, P3 and P4 calculated at M06-2X/aug-cc-pVDZ level. For the sake of clarity only the bond critical points are shown. Arrows point the intermolecular bond critical points.

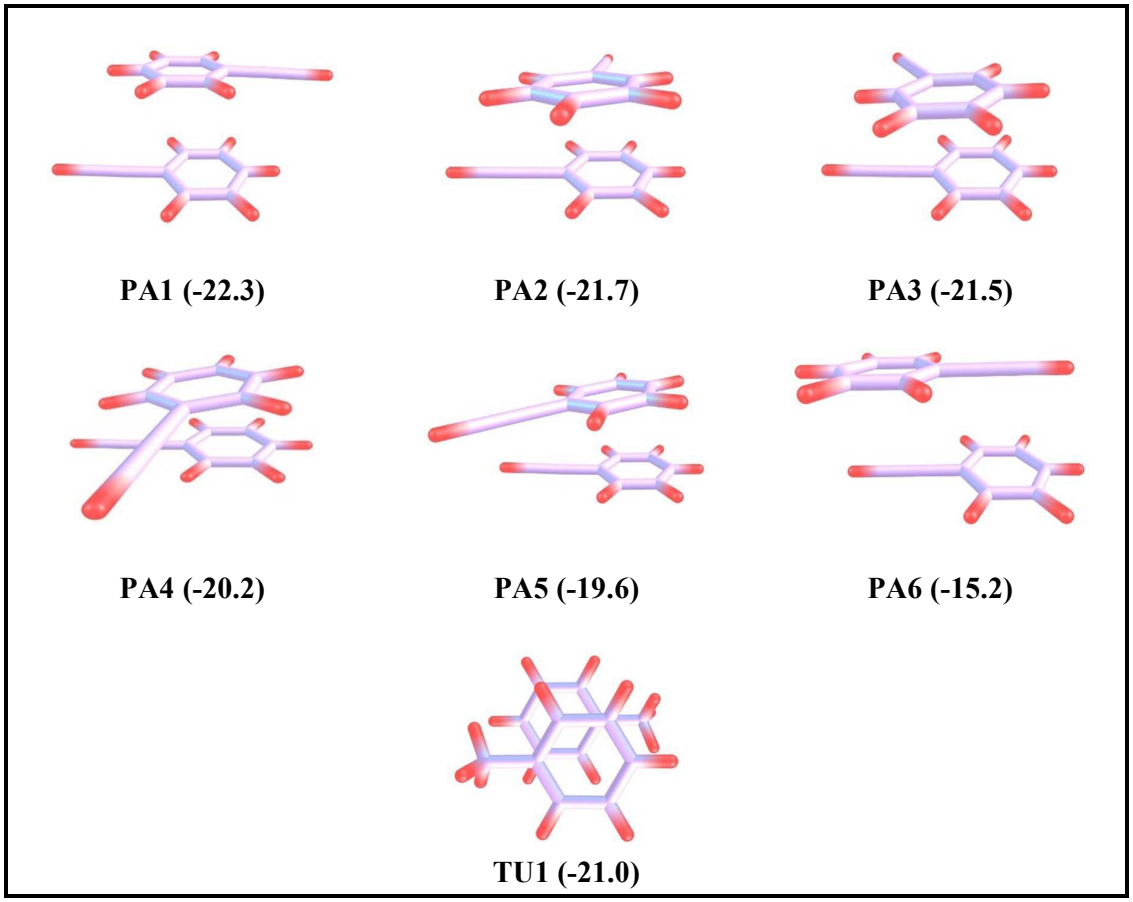

Fig. 7. Structures of π-stacked phenylacetylene dimers and toluene dimer optimized at M06-2X/aug-cc-pVDZ level. ZPE and BSSE corrected stabilization energies (kJ mol^{-1}) at ωB97X-D/aug-cc-pVDZ level of theory are shown in parenthesis (see Table 4).

Infrared spectrum of the size-selected propargylbenzene dimer suggest formation of a π-stacked dimer.